Progress In Electromagnetics Research C, Vol. 140, 117-126, 2024

(Received 7 November 2023, Accepted 7 January 2024, Scheduled 20 January 2024)

PMSM Parameter Identification Based on Chaotic Adaptive Search Grey Wolf Optimization Algorithm

Yang Zhang[1], Ziying Liu[1], Mingfeng Zhou[1], Sicheng Li[1], Jiaxuan Li[1], and Zhun Cheng[2*]

[1]*Hunan University of Technology, Zhuzhou 412007, China*
[2]*Hunan Railway Professional Technology College, Zhuzhou 412001, China*

ABSTRACT: Aiming at the problems of poor population diversity, slow speed of late identification, and low identification accuracy of traditional grey wolf algorithm (GWO), a chaotic adaptive search grey wolf optimization algorithm (CASGWO) for parameter identification of permanent magnet synchronous motor is proposed in this paper. Firstly, multiple low-dimensional chaotic mappings are combined; a composite chaotic system Tent-Logistic-Cosine is obtained; uniform populations are generated. So the population diversity and global search capability are improved. Then a segmented nonlinear search method is proposed, where the nonlinear decay factor quickly converges to the vicinity of the optimal solution in the first segment and slows down the convergence rate for local search in the second segment. Thus, the convergence rate is accelerated while the local search capability is enhanced. Finally, the adaptive inertia weights are adjusted according to the fitness values of different wolf pack iterations, and ω wolves approach the leader wolf pack with smaller fitness values at a faster speed. Therefore, the speed of search is again improved, and the local search ability of the algorithm is again enhanced. Experiments show that when identifying multiple parameters of resistance, inductance, and permanent magnet flux of a permanent magnet synchronous motor, the CASGWO method has good global and local search capability, with faster identification speed and higher identification accuracy than the traditional grey wolf algorithm.

1. INTRODUCTION

Permanent magnet synchronous motor (PMSM) is widely used in robotics, new energy vehicles, and wind power generation due to their high efficiency an high power density [1–4]. The accuracy of parameter identification has a significant impact on the control performance, speed regulation, and control prediction of PMSM [5–7]. However, the parameters of PMSMs including stator resistance, stator inductance, and permanent magnet flux are affected by various factors such as the degree of magnetic saturation, temperature, and load perturbation during the actual operation [8–10]. Varying parameters can lead to the reduction of control performance and safety reliability of the motor. Therefore, the accurate identification of multiple parameters of PMSM is the key to improve the control quality of permanent magnet synchronous motor control system.

To achieve multi-parameter identification of PMSM, many scholars have proposed different methods for online parameter identification. The online parameter identification methods include recursive least squares (RLS), extended Kalman filter (EKF), model reference adaptive system (MRAS), and intelligent algorithms. The method in [11] presents a dynamic decoupling control method for permanent magnet synchronous motors in a brake-by-wire system, but only inductance and magnetic chain can be identified. The method presented in [12] combines EKF and LS with consideration of magnetic saturation, and identifies only the magnetic chain and inductance in a stepwise manner, which takes a long time. The method in [13] proposes a multi-parameter estimation method using a model-referenced adaptive system to estimate and continuously update the stator resistance and rotor magnetic chain in a closed-loop manner, thus eliminating the sensitivity to multi-parameter variations at low speed.

In addition to the traditional methods, intelligent algorithms have emerged in recent years to be used to identify the parameters of PMSM, and many scholars have improved different intelligent algorithms. In [14], a parameter identification method based on an improved cuckoo search algorithm is proposed. Cloud fuzzy logic and adaptive variable step size methods are employed to change the parameters of the cuckoo search algorithm, and the local and global optimisation search capability is improved. An improved fuzzy particle swarm algorithm is proposed in [15], where the velocity of each particle is changed from being affected only by the optimal particle to being affected by the surrounding particles. Convergence factors are introduced, and this method ensures the accuracy of the algorithm's identification and the convergence performance of the algorithm, which is capable of identifying the four parameters of the PMSM simultaneously. In [16], a new variable step size neural network algorithm was designed to introduce a velocity factor in the step function to ensure the performance of the recognition algorithm at different speeds. The recognition process is faster and more stable. The presented method in [17] considers the voltage source inverter nonlinearity and designs an immune operator based on chaotic logic. An adaptive speed particle swarm algorithm was proposed in [18] to control the

* Corresponding author: Zhun Cheng (120277982@qq.com).

PMSM and optimise the objective function to find the best parameters in the weak magnetic region and to achieve the minimum error of the controller. The dynamic self-learning particle swarm optimisation algorithm in [19] introduces a nonlinear multi-scale interactive learning operator to speed up the convergence of the particles, and it is capable of holistically tracking the electrical parameters, mechanical parameters and VSI of the PMSM transmission. In [20], grey wolf optimization algorithm and particle swarm optimization algorithm were combined, and multiple sets of test functions were used to compare the performance of the algorithms, which proved to perform well in terms of quality of solution, stability of the solution, speed of convergence, and the ability to find a globally optimal solution. Improved grey wolf algorithm using grouping strategy and convergence factor with nonlinear decay was proposed in [21] to identify the parameters of generator excitation system. The grey wolf optimisation algorithm in [22] was used to perform state feedback control, and the results show that the control results have the advantage of fast response and no overshooting. The grey wolf algorithm and model reference adaptive were combined in [23], using the grey wolf optimization algorithm to optimize the proportional-integral controller parameters for the speed adaptive law obtained from MRAS which can obtain better speed performance.

In order to improve the convergence speed and recognition accuracy of GWO and to improve the balance between its local and global search abilities, a parameter recognition method of PMSM based on chaotic adaptive search grey wolf optimisation algorithm is proposed. The specific implementation method is as follows:

1) According to the mathematical model of PMSM, the negative sequence current with $i_d = -2$ is injected into the d-axis to construct the full rank equation containing the parameters to be identified.
2) Multiple low-dimensional chaotic mappings are composited to generate a high-dimensional Tent-Logistic-Cosine chaotic system, and the population generated by the composite chaotic system ensures the diversity and traversal of the initial population of GWO. As a result, the algorithm's global search capability and recognition speed are enhanced.
3) A nonlinear decay factor is introduced into the GWO algorithm for segmented nonlinear search of the population, and the convergence speed at different stages is flexibly adjusted, with rapid convergence in the early stage and decelerated search in the later stage. The accuracy and speed of search are improved.
4) According to the distance and position of different leader wolves and ω wolves, judge the size of the leadership ability of the leader wolves, calculate the value of iterative fitness, and adaptively adjust the iterative inertia weights. The local search ability and search speed of wolf packs are improved.
5) The final experimental results show that the method is able to identify the resistance, inductance, and magnetic flux parameters of PMSM simultaneously online. Compared with the traditional GWO, the convergence speed is faster, the recognition accuracy stronger, and it has good global and local search capability.

The remaining subsections of the paper are organised as follows. The mathematical model and full rank equations of the permanent magnet synchronous motor are constructed in Section 2. The principle and process of the method used are presented in Section 3. The fitness function is constructed in Section 4, and the process and implementation of the parameter identification of the described method are described. In Section 5, the experimental conditions and experimental platform are described, and a validation analysis is carried out based on the experiments. In Section 6, conclusions are given based on the theory and experiments.

2. MATHEMATICAL MODEL OF PMSM

Neglecting the effect of the core saturation loss of the PMSM, the voltage equation of the PMSM under the d-q coordinate system is expressed as:

$$\begin{cases} u_d = R_s i_d + L_d \frac{di_d}{dt} - \omega_n L_q i_q \\ u_q = R_s i_q + L_q \frac{di_q}{dt} + \omega_n L_d i_d + \omega_n \psi_m \end{cases} \tag{1}$$

where R_s denotes the stator resistance; L_d and L_q denote the d-axis inductance and q-axis inductance; $L_d = L_q = L_s$; i_d and i_q denote the stator current; ω_n denotes the electrical angular velocity; ψ_m denotes the permanent magnet flux; u_d and u_q denote the stator voltage.

When the motor is running steadily the current change is very small, so the current differential component in (1) is close to 0 and can be ignored:

$$\begin{cases} \frac{di_d}{dt} = 0 \\ \frac{di_q}{dt} = 0 \end{cases} \tag{2}$$

Then (1) can be simplified as:

$$\begin{cases} u_d = R_s i_d - \omega_n L_q i_q \\ u_q = R_s i_q + \omega_n L_d i_d + \omega_n \psi_m \end{cases} \tag{3}$$

The negative sequence current with $i_d = -2$ is injected in the d-axis, and the fourth order full rank equation is obtained as:

$$\begin{cases} u_{d0}(k) = -\omega_{n0}(k) L_q i_{q0}(k) \\ u_{q0}(k) = R_s i_{q0}(k) + \omega_{n0}(k) \psi_m \\ u_{d2}(k) = R_s i_{d2}(k) - \omega_{n2}(k) L_q i_{q2}(k) \\ u_{q2}(k) = R_s i_{q2}(k) + \omega_{n2}(k) L_d i_{d2}(k) + \omega_{n2}(k) \psi_m \end{cases} \tag{4}$$

where the variable with subscript 0 represents the voltage and current of the d-axis and q-axis sampled at $i_d = 0$. The variable with subscript 2 represents the voltage and current of the d-axis and q-axis sampled at $i_d = -2$.

The k-th sampled data of current, voltage, and electrical angular velocity collected under the two operating conditions of the motor are shown in Figure 1.

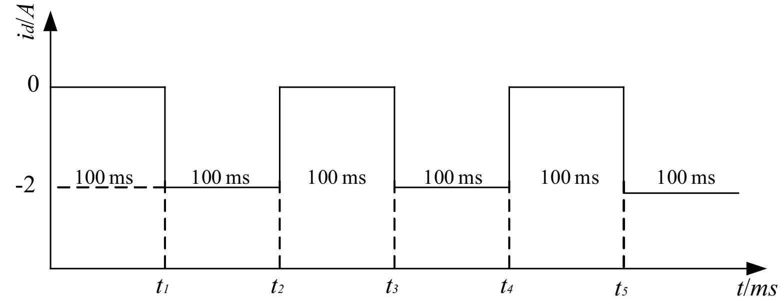

FIGURE 1. Data sampling diagram.

3. CHAOTIC ADAPTIVE SEARCH GREY WOLF OPTIMISATION ALGORITHM

3.1. Grey Wolf Optimization (GWO)

The GWO algorithm, a meta-heuristic optimization algorithm by simulating grey wolf packs for collaborative predation, was proposed in 2014 by by Seyedali Mirjalili et al. in [24]. It is characterized by a simple structure, a few parameters to be adjusted, and easy to implement. The existence of adaptive convergence factors and information feedback mechanisms can achieve a balance between local optimisation and global search, thus providing good performance in terms of problem solving accuracy and convergence speed.

The core idea of the grey wolf algorithm is to simulate the hierarchy of a wolf pack, with α, β, and δ wolves leading ω wolves to encircle, pursue, and attack the prey. Among them, α, β, and δ wolves represent the optimal, suboptimal, and third-best solutions, respectively, and ω wolves are moved so as to achieve the global search.

In GWO, the lead wolf changes position to lead the pack to encircle the prey, updating the position according to the following formula:

$$\begin{cases} \vec{D} = \left|\vec{C} \cdot \vec{X}_m(k) - \vec{X}(k)\right| \\ \vec{X}(k+1) = \vec{X}_m(k) - \vec{A} \cdot \vec{D} \end{cases} \tag{5}$$

$\vec{D}$ is the distance between the grey wolf and the prey; $\vec{X}_m$ and $\vec{X}$ are the position vectors of the prey and the grey wolf respectively; k is the number of current iterations; $\vec{A}$ and $\vec{C}$ are the change coefficient matrices in each iteration. The calculation formulas are designed as:

$$a = 2\left(1 - \frac{t}{M}\right) \tag{6}$$

$$\begin{cases} \vec{A} = a\left(2\vec{r}_1 - 1\right) \\ \vec{C} = 2\vec{r}_2 \end{cases} \tag{7}$$

where $\vec{r}_1$ and $\vec{r}_2$ are two vectors of random numbers with values in [0, 1]; t is the number of iterations; M is the maximum number of iterations, and the values decrease linearly from 2 to 0 as the number of iterations increases.

Then the distance between wolves is calculated as:

$$\begin{cases} \vec{D}_1 = \left|\vec{C}_1 \cdot \vec{X}_\alpha - \vec{X}\right| \\ \vec{D}_2 = \left|\vec{C}_2 \cdot \vec{X}_\beta - \vec{X}\right| \\ \vec{D}_3 = \left|\vec{C}_3 \cdot \vec{X}_\delta - \vec{X}\right| \end{cases} \tag{8}$$

$\vec{D}_1$, $\vec{D}_1$, and $\vec{D}_1$ represent the distance of other individual grey wolves from the α, β, and δ packs, respectively. $\vec{X}$ is the current position of the grey wolf.

The location and direction of wolf pack adjustments are expressed as:

$$\begin{cases} \vec{X}_1 = \left|\vec{X}_\alpha - \vec{A}_1 \cdot \vec{D}_1\right| \\ \vec{X}_2 = \left|\vec{X}_\beta - \vec{A}_2 \cdot \vec{D}_2\right| \\ \vec{X}_3 = \left|\vec{X}_\delta - \vec{A}_3 \cdot \vec{D}_3\right| \end{cases} \tag{9}$$

where $\vec{X}_1$, $\vec{X}_2$, and $\vec{X}_3$ denote the step length and direction of approach to the α, β, and δ packs, respectively.

$\vec{X}_{(t+1)}$ denotes the position of the individual grey wolf that needs to be adjusted. Here the mean value is expressed as:

$$\vec{X}_{(t+1)} = \frac{\vec{X}_1 + \vec{X}_2 + \vec{X}_3}{3} \tag{10}$$

A schematic diagram for the way of updating the position of a grey wolf is shown in Figure 2.

3.2. Tent-Logistic-Cosine Combined Chaotic Grey Wolf Algorithm (CGWO)

Swarm intelligence algorithms in meta-heuristic algorithms generally use a random population generation strategy, but the population is usually disordered which can lead to uneven distribution and poor diversity of the initial population. The distribution state of the population directly determines the process of wolf search, and random, unevenly distributed as well as regular populations will limit the search range of wolves. This has a great impact on the accuracy of identification. Chaotic mapping has good traversal and randomness. To improve the diversity and uniformity of the population, separate low-dimensional chaotic mappings are employed to initialise the population. In this paper, multiple low-dimensional chaotic mappings are

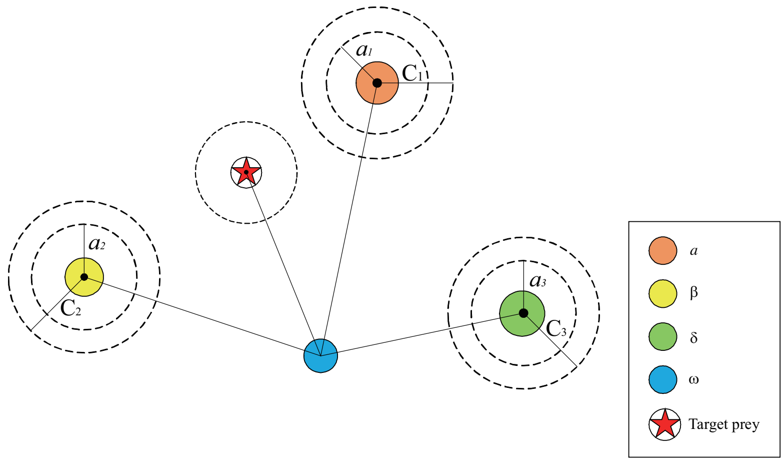

FIGURE 2. Updated schematic of grey wolf location.

combined to generate composite chaotic systems with better diversity. A CGWO algorithm based on the Tent-Logistic-Cosine composite chaotic system is proposed to initialise the population, and its expression is devised as:

$$x_{(k+1)}=\begin{cases}\cos(\pi(2cx_{(k)}+4(1-c)x_{(k)}\\(1-x_{(k)})-0.5)), \quad x_{(k)}<0.5\\\cos(\pi(2c(1-x_{(k)})+4(1-c)x_{(k)}\\(1-x_{(k)})-0.5)), \quad x_{(k)}\geq 0.5\end{cases}, \quad c\in[0,1] \tag{11}$$

The composite chaotic system was added to the grey wolf algorithm to generate diverse and evenly distributed populations. The location of the lead pack was evenly dispersed; the number of hunting paths increased; the hunting range increased; the location of prey was more accurately localised; consequently, the global search ability and convergence speed of the pack was improved.

3.3. CNGWO Algorithm Based on Nonlinear Decay Factor

In the standard GWO algorithm, the convergence factor a determines the predation speed of the wolves, and the value of the convergence factor a decreases linearly from 2 to 0. Since the search process of the GWO algorithm is nonlinear and highly complex, the linear decay strategy is not flexible. Therefore, this paper proposes a new nonlinear exponential decay factor strategy to search in segments according to the progress of convergence. The nonlinear decay factor converges quickly to the neighbourhood of the optimal solution by exponential decay in the first segment and slows down the convergence by quadratic decay in the second segment for local search, and the arithmetic is expressed as:

$$T=\frac{t}{M} \tag{12}$$

$$a_{(k+1)}=\begin{cases}a_i+(a_f-a_i)e^{-KT},\\0<T\leq 0.7\\-\frac{100}{9}e^{-0.7K}(T^2-1.4T+0.4),\\0.7<T<1\end{cases} \tag{13}$$

Combining (6), (7), (12), (13) and substituting into (5), the equation of the lead wolf pack can be updated as:

$$\vec{X}_{(k+1)}=\begin{cases}\overrightarrow{X_m}(k)-2(1+e^{-KT})(2\vec{r_1}-1)\\\left|2\vec{r_2}\overrightarrow{X_m}(k)-\vec{X}_{(k)}\right|, \quad 0\leq T\leq 0.7\\\overrightarrow{X_m}(k)+\frac{200}{9}e^{-0.7K}(T^2-1.4T+0.4)\\\left|2\vec{r_2}\overrightarrow{X_m}(k)-\vec{X}_{(k)}\right|, \quad 0.7\leq T\leq 1\end{cases} \tag{14}$$

t represents the current number of iterations; M is the maximum number of iterations; T is the ratio of t to M; K is a constant with a value greater than 1 and can be adjusted to the segmentation threshold; a_i and a_f represent the initial and termination values of the control parameter a, respectively, with the initial value set to 2 and the termination value set to 0.

For the speed of wolf hunting and searching to take segmented convergence, wolves can flexibly regulate the speed and path of searching. The pre-hunting period needs to be quick to narrow down the hunt and speed up the search. In the post-hunting period it is necessary to search more carefully and more precisely at a localised scale to ensure that the prey is accurately located. The value of K can adjust the value of the segmentation point; the larger the value of K is, the smaller the critical value is; the first segment converges faster; the second segment slows down; and the local search scope is reduced. The smaller the value of K is the larger the critical value is; the first segment searches slower; the second segment searches faster; and the local search scope is enlarged.

3.4. CASGWO Algorithm Based on Chaotic Adaptive Search

From (11), the GWO algorithm hunts for the optimal solution, the second best solution, and the third best solution represented by α, β and δ wolves, respectively, using the average value. However, since the fitness values of the solutions are different, the use of the average value does not reflect the real prey location. In order to approach the prey more quickly and accurately, an adaptive inertia weighting method is proposed. ω wolves approach the leader wolf with a smaller value of fitness; the search for optimality approaches the optimal solution at a

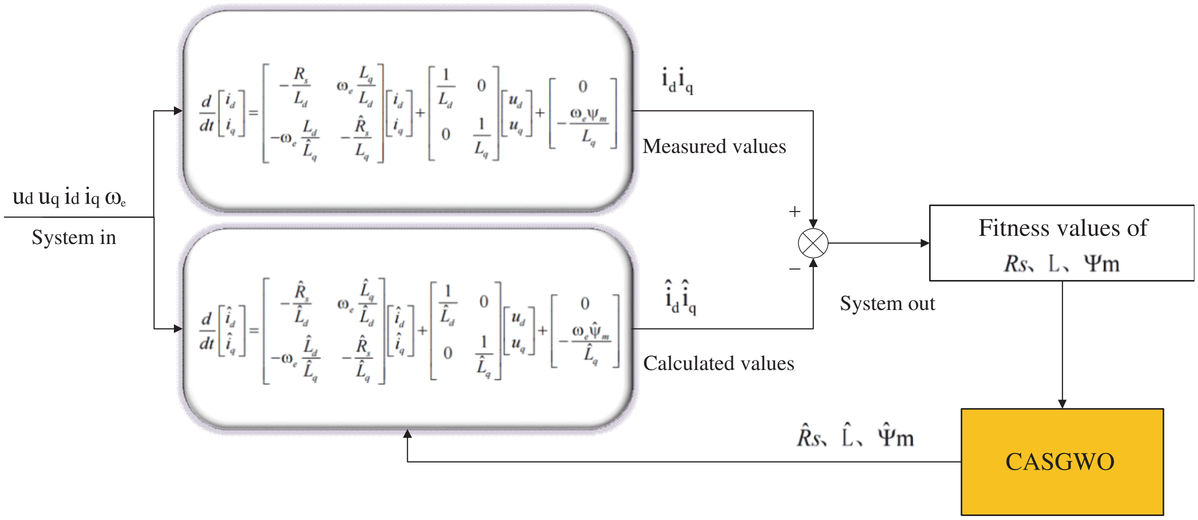

FIGURE 3. Schematic diagram for identification.

faster speed; and the arithmetic is designed as:

$$\begin{cases} f=|f_1|+|f_2|+|f_3| \\ w_1=\frac{|f_3|}{f},\ w_2=\frac{|f_2|}{f},\ w_3=\frac{|f_1|}{f},\ f\neq 0 \\ w_1=w_2=w_3=\frac{1}{3},\ f=0 \end{cases} \tag{15}$$

where f_1, f_2, and f_3 represent the fitness values of α, β, and δ wolves, respectively, and w_1, w_2, and w_3 represent the adaptive inertia weighting coefficients associated with the fitness.

According to (15), Equation (10) for grey wolf hunting can be updated as:

$$\vec{X}_{(t+1)}=\begin{cases} w_1\vec{X}_1+w_2\vec{X}_2+w_3\vec{X}_3, & f\neq 0 \\ \frac{\vec{X}_1+\vec{X}_2+\vec{X}_3}{3}, & f=0 \end{cases} \tag{16}$$

Due to the different positions of α, β, and δ wolves, the movement of ω wolves according to the command of the leader wolf is affected differently; however, adaptive inertia weights can help ω wolves to judge the position of their prey more accurately. Each time the position of the moving leader is updated, the adaptability value is updated simultaneously. The wolves can instantly adjust the direction of their search towards the leader closer to the prey to speed up the hunt.

4. EXPERIMENTAL VERIFICATION

Parameter identification can be translated into regulating the adjustable model by comparing the magnitude of the error between the adjustable model and actual model, and ultimately it is transformed into an optimisation problem. The principle of parameter identification is expressed in Figure 3. The system control diagram is shown in Figure 4.

The control of the PMSM ultimately boils down to the control of the two-phase currents, so the accuracy of the discrimination values can be judged by constructing the fitness function using the errors of the d-axis currents and q-axis currents. A smaller value of fitness indicates a more accurate discrimination value and is represented as:

$$Fitness = c_1(i_{d0}-\hat{i}_{d0})^2+c_2(i_{q0}-\hat{i}_{q0})^2 + c_3(i_{d1}-\hat{i}_{d1})^2+c_4(i_{q1}-\hat{i}_{q1})^2 \tag{17}$$

where c_1, c_2, c_3, c_4 are constants in the range (0, 1).

The steps to improve the grey wolf algorithm are:

Step 1: Acquisition of current, voltage, and angular velocity electrical signals at $i_d=-2$ and $i_d=0$;

Step 2: Tent-Logistic-Cosine chaotic mapping is used to generate initialised populations;

Step 3: Calculate the nonlinear convergence factor a according to (12) and (13), generate matrix A, matrix C according to (6) and (7), and calculate the distance with position of each wolf pack according to (8) and (9) as well as record them;

Step 4: Calculate the fitness value of each wolf pack, calculate the inertia weight and update the ω wolf pack position according to (16) and (17), and replaced with the values of α wolf pack, β wolf pack, and δ wolf pack if they are smaller than the fitness value of the previous iteration, and return to step 3 to update if they are larger than the fitness value of the previous iteration;

Step 5: The iteration is completed, and the optimal solution is output.

The flowchart of CASGWO is shown in Figure 5.

5. EXPERIMENTAL RESULTS AND ANALYSIS

In order to verify the feasibility of the proposed method, the hardware experimental platform RT-LAB is used in this paper, as shown in Figure 6. The RT-LAB hardware in the loop system configuration is shown in Figure 7 and includes TMS320F2812 DSP controller, RT-LAB (OP5600) simulator, motor drive model built in RT-LAB, and the host computer. The DSP controller uses TMS320F2812 as the running algorithm and RT-LAB to implement the inverter and permanent magnet synchronous motor. The sampling frequency of the experimental system is 10 kHz. The parameters of the PMSM are shown in Table 1.

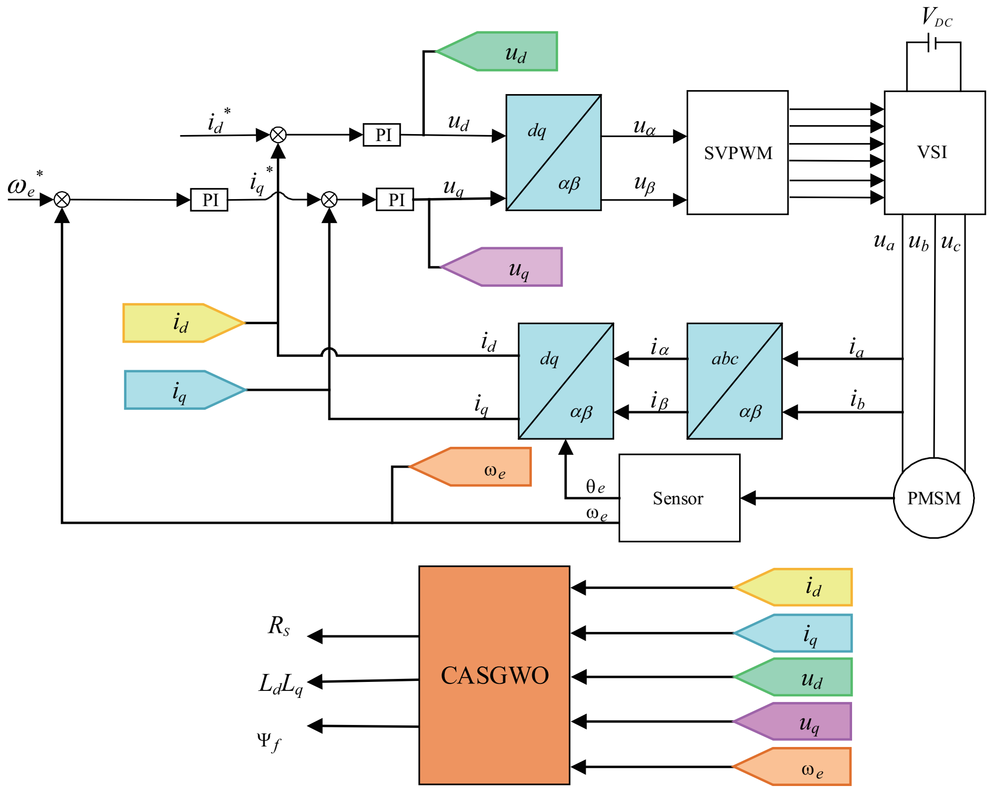

FIGURE 4. Diagram of system control.

TABLE 1. Motor parameters.

Parameter	Value
Pole Pairs	4
Rated Speed/rpm	1000
Rated Torque/N · m	12
Moment of Inertia/(kg · m^2)	0.003
Stator resistance/Ω	1
D-axis inductance/mH	5.6
Q-axis inductance/mH	5.6
Permanent magnet flux/Wb	0.2

In order to effectively compare the experimental results of the algorithms, the initial populations of the tested algorithms were all set to 50, and the boundary values of the algorithms' to be recognised values were set the same. The maximum number of iterations is the ratio of the running time to the sampling time. The experimental running time is 0.3 s, and the number of currents, voltages, and rotational speeds of the d-axis and q-axis are sampled. To prevent errors due to chance results, GWO, CGWO, CNGWO, and CASGWO were run 10 times, and the averages of each algorithm were taken as the outputs.

The identified results of the four methods are shown in Figures 8–10. The identified stator resistance is shown in Figure 8. The experimental results can be analysed in terms of both the magnitude of the error in the curves and the convergence time. The errors of GWO, CGWO, CNGWO, and CASGWO are 3.80%, 3.10%, 2.58%, and 1.50%, and the convergence times are 0.27 s, 0.18 s, 0.11 s, and 0.09 s, respectively. The error of the identification decreases in turn and the speed of convergence is gradually accelerated. The CASGWO has the shortest recognition time and the highest recognition accuracy.

The identified stator inductance is shown in Figure 9. GWO is slow to recognise and easy to fall into local optimum, and the improved algorithm is significantly faster. The convergence time is 0.2 s for GWO, 0.13 s for CGWO, 0.08 s for CNGWO, and 0.07 s for CASGWO. CASGWO identifies the fastest, with a discrimination error of 0.89%, and the discrimination value is closest to the reference value.

The recognised magnetic flux is shown in Figure 10. CASGWO tends to stabilise in the shortest time with the smallest amount of overshooting, reflecting good recognition speed and robust performance. The convergence time of GWO is 0.24 s and the discrimination error is 3.10%. Compared to GWO, CGWO has a convergence time of 0.18 s with an error reduction of 0.35%; CNGWO has a convergence time of 0.14 s with an error reduction of 1.80%; and CASGWO has a convergence time of 0.12 s with an error reduction of 2.95%.

The experimental discrimination averages and convergence times for the four methods are shown in Table 2.

Based on the experimental figures and data, it can be seen that the maximum errors of GWO, CGWO, CNGWO, and CASGWO identification are 3.80%, 3.10%, 2.58%, and 1.50%,

TABLE 2. Experimental results.

Parameter	GWO	CGWO	CNGWO	CASGWO
R/Ω	1.0380	1.0310	1.0258	1.015
Error/%	3.80%	3.10%	2.58%	1.50%
Time/s	0.27	0.18	0.11	0.09
L_S/mH	5.760	5.696	5.689	5.650
Error/%	2.86%	1.71%	1.58%	0.89%
Time/s	0.20	0.13	0.08	0.07
Ψ_f/Wb	0.2162	0.2055	0.2026	0.1997
Error/%	3.10%	2.75%	1.30%	0.15%
Time/s	0.24	0.18	0.14	0.12

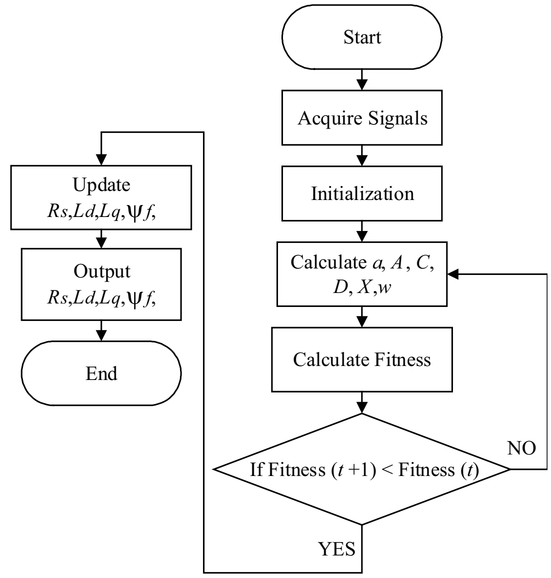

FIGURE 5. CASGWO flowchart.

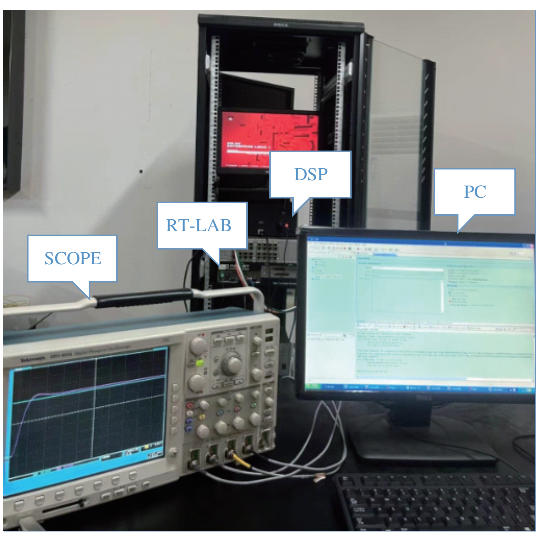

FIGURE 6. RT-LAB experimental platform.

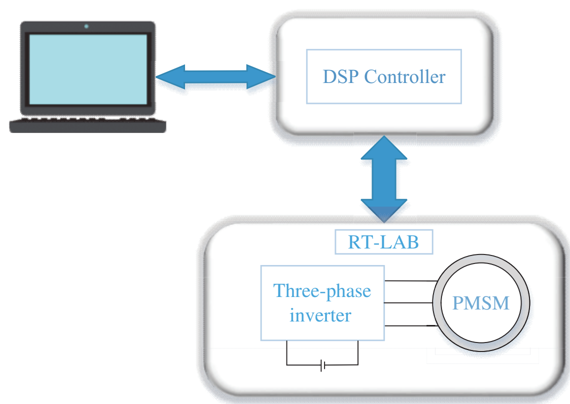

FIGURE 7. RT-LAB hardware in the loop system configuration diagram.

(a)

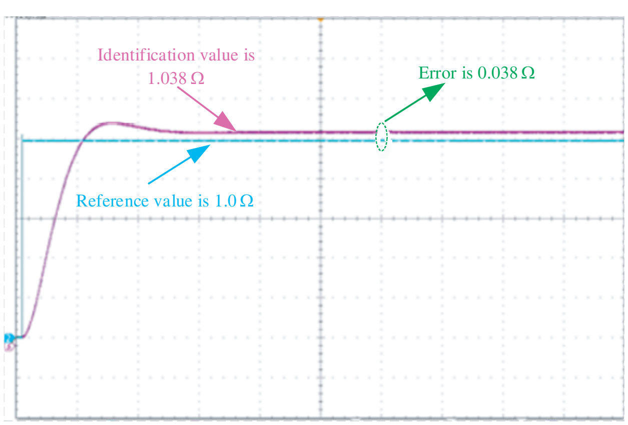

GWO (100 ms/div)

(b)

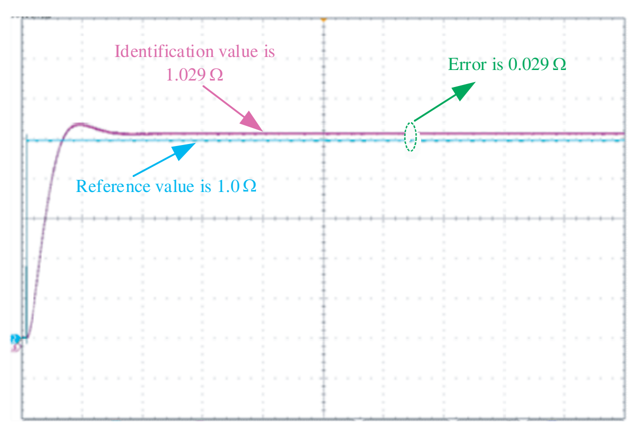

CGWO (100 ms/div)

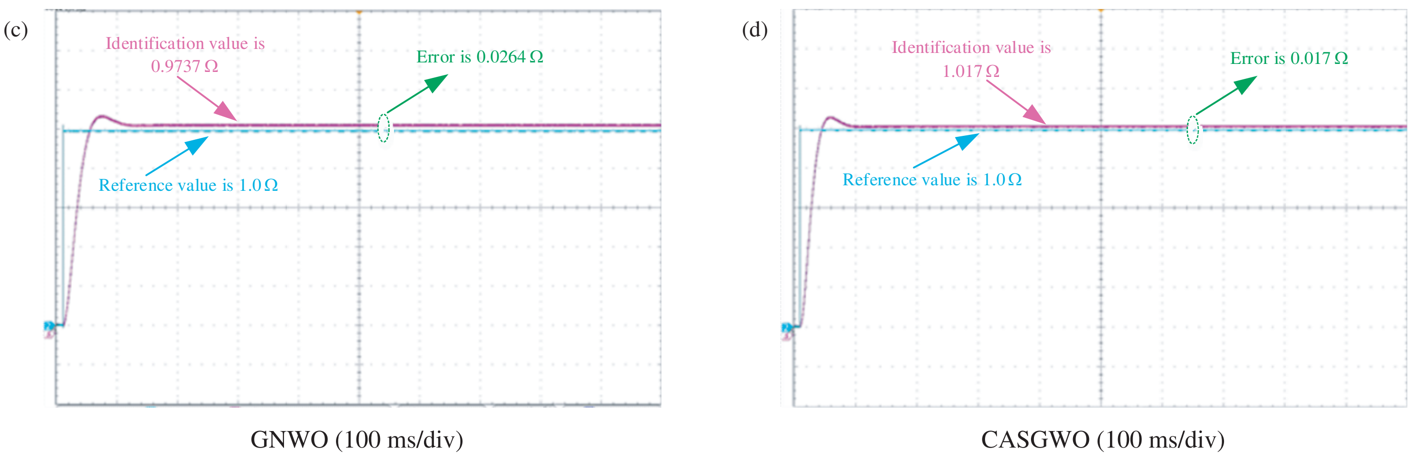

FIGURE 8. Identification curves for stator resistance.

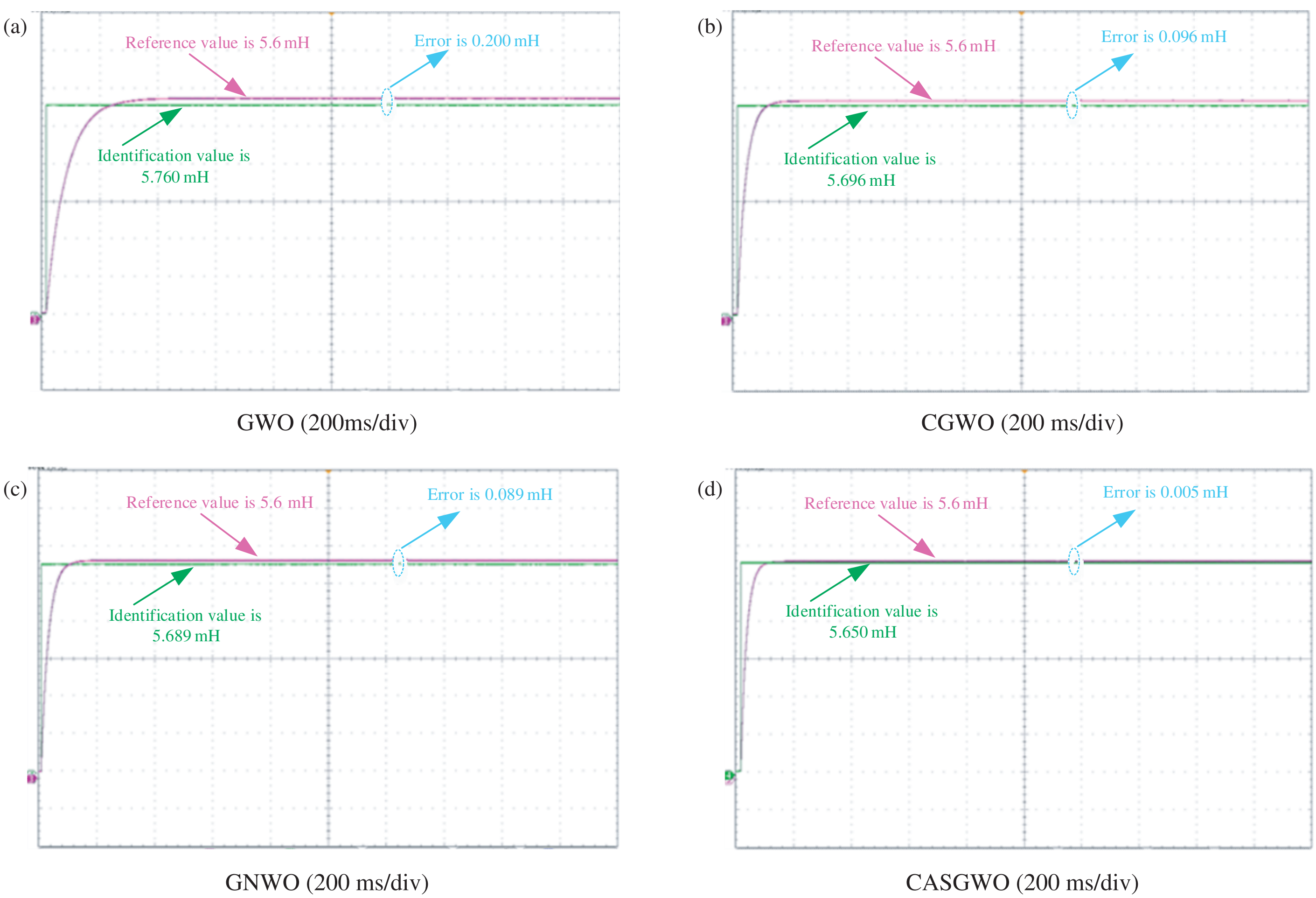

FIGURE 9. Identification curves for inductance.

and the minimum errors are 2.86%, 1.71%, 1.30%, and 0.15%, respectively. The minimum convergence times are 0.20 s, 0.13 s, 0.08 s, and 0.07 s. The improved CGWO, CNGWO, and CASGWO recognition accuracy and speed are improved. Among them, CASGWO has the best performance with a maximum identification error of 1.50% and a minimum of 0.15%. The convergence time is less than 0.12 s. From the experimental results, it can be concluded that CASGWO has good robustness and better identification speed and identification accuracy than the other three algorithms.

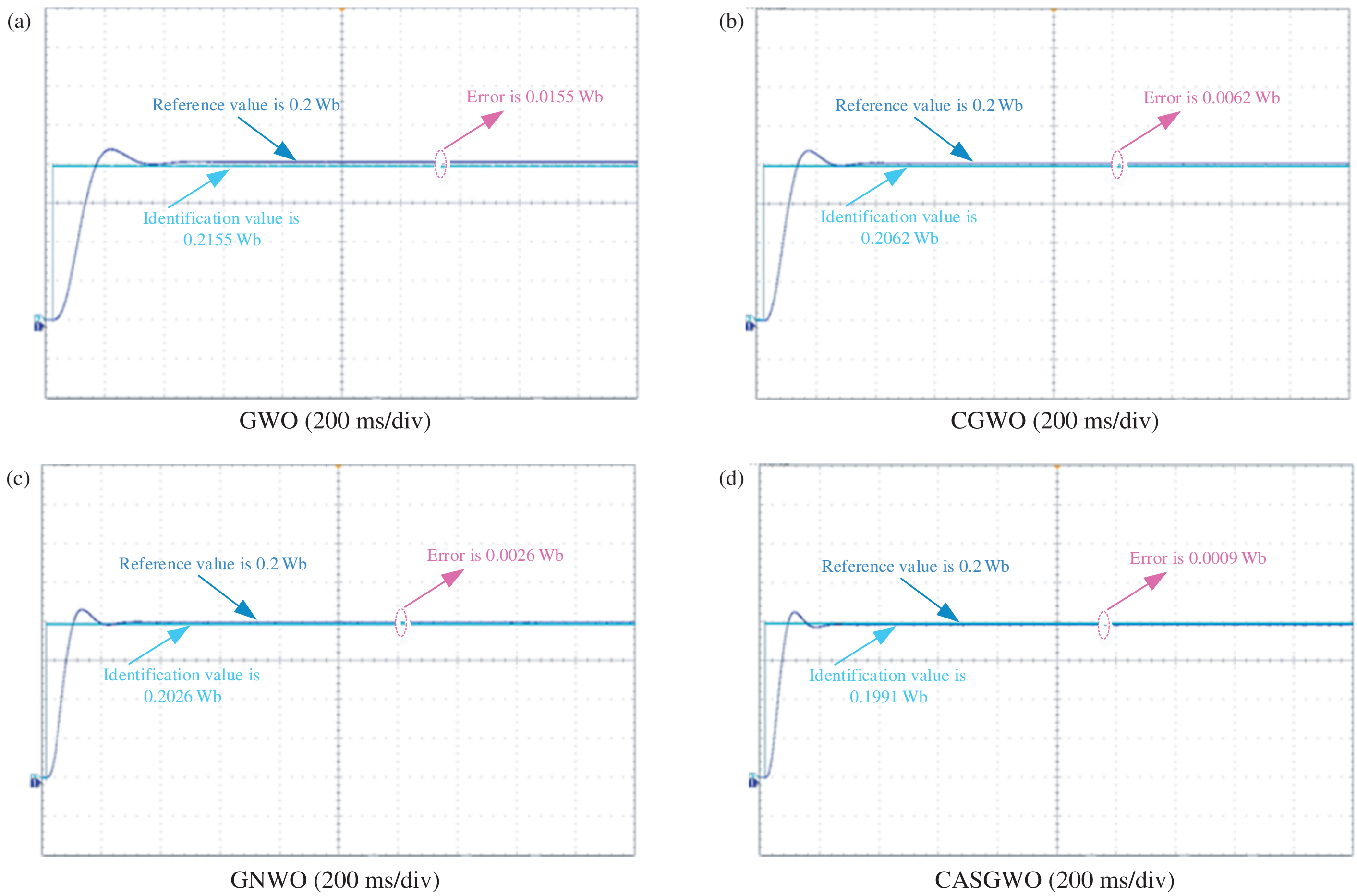

FIGURE 10. Recognition curves for magnetic flux.

6. CONCLUSION

In this paper, for the problems of poor population diversity, long convergence time and poor recognition accuracy of the grey wolf algorithm, a parameter recognition method of CASGWO is proposed, and it can achieve the online recognition of resistance, magnetic flux, as well as inductance of PMSM. The following conclusions can be drawn from the theoretical and experimental validation results:

1) The improved CGWO, CNGWO, and CASGWO have better population diversity and improved global and local search capabilities. As a result, the accuracy and speed of the recognition are improved. The minimum errors of GWO, CGWO, CNGWO, and CASGWO recognition are 2.86%, 1.71%, 1.30%, and 0.15%, respectively, and the shortest convergence times are 0.20 s, 0.13 s, 0.08 s, and 0.07 s, respectively. Among them, CASGWO achieves the best identification.

2) The recognition time of the CASGWO algorithm is controlled within 0.12 s, and the recognition error is less than 1.50%. Compared with GWO, the errors of PMSM resistance, inductance, and magnetic chain identification are reduced by 2.30%, 1.97%, and 2.95%, and the identification time is shortened by 0.18 s, 0.13 s and 0.12 s, respectively. The CASGWO algorithm has the advantages of fast identification speed, high identification accuracy, and good robustness.

ACKNOWLEDGEMENT

This work was supported by the Natural Science Foundation of Hunan Province of China under Grant Number 2023JJ50191, Educational Commission of Hunan Province of China under Grant Number 21B0552.

REFERENCES

[1] Fan, Z.-X., S. Li, and R. Liu, "ADP-based optimal control for systems with mismatched disturbances: A PMSM application," *IEEE Transactions on Circuits and Systems II: Express Briefs*, Vol. 70, No. 6, 2057–2061, Jun. 2023.

[2] Wu, L. and Z. Lyu, "Harmonic injection-based torque ripple reduction of PMSM with improved DC-link voltage utilization," *IEEE Transactions on Power Electronics*, Vol. 38, No. 7, 7976–7981, Jul. 2023.

[3] Wei, Y., F. Wang, H. Young, D. Ke, and J. Rodríguez, "Autoregressive moving average model-free predictive current control for PMSM drives," *IEEE Journal of Emerging and Selected Topics in Power Electronics*, Vol. 11, No. 4, 3874–3884, Aug. 2023.

[4] Chen, Y., C. Liu, S. Liu, and Y. Liu, "Predictive control scheme with adaptive overmodulation for a five-leg VSI driving dual PMSMs," *IEEE Transactions on Industrial Electronics*, Vol. 71, No. 1, 71–81, Jan. 2024.

[5] Liu, J., J. Yang, S. Li, and X. Wang, "Single-loop robust model predictive speed regulation of PMSM based on exogenous signal preview," *IEEE Transactions on Industrial Electronics*, Vol. 70,

No. 12, 12 719–12 729, Dec. 2023.

[6] Moon, H.-T., H.-S. Kim, and M.-J. Youn, "A discrete-time predictive current control for PMSM," *IEEE Transactions on Power Electronics*, Vol. 18, No. 1, 464–472, Jan. 2003.

[7] Zhang, H., T. Fan, L. Meng, J. Guo, and X. Wen, "Polynomial estimation of flux linkage for predictive current control in PMSM," *IEEE Journal of Emerging and Selected Topics in Power Electronics*, Vol. 10, No. 5, 6112–6122, Oct. 2022.

[8] Wang, Q., G. Wang, N. Zhao, G. Zhang, Q. Cui, and D. Xu, "An impedance model-based multiparameter identification method of PMSM for both offline and online conditions," *IEEE Transactions on Power Electronics*, Vol. 36, No. 1, 727–738, Jan. 2021.

[9] Grobler, A. J., S. R. Holm, and G. van Schoor, "Empirical parameter identification for a hybrid thermal model of a high-speed permanent magnet synchronous machine," *IEEE Transactions on Industrial Electronics*, Vol. 65, No. 2, 1616–1625, Feb. 2018.

[10] Rafaq, M. S., F. Mwasilu, J. Kim, H. H. Choi, and J.-W. Jung, "Online parameter identification for model-based sensorless control of interior permanent magnet synchronous machine," *IEEE Transactions on Power Electronics*, Vol. 32, No. 6, 4631–4643, Jun. 2017.

[11] Zhu, Z., X. Wang, B. Yan, L. Li, and Q. Wu, "A dynamic decoupling control method for PMSM of brake-by-wire system based on parameters estimation," *IEEE/ASME Transactions on Mechatronics*, Vol. 27, No. 5, 3762–3772, Oct. 2022.

[12] Liu, Z., G. Feng, and Y. Han, "Extended-kalman-filter-based magnet flux linkage and inductance estimation for PMSM considering magnetic saturation," in *2021 36th Youth Academic Annual Conference of Chinese Association of Automation (YAC)*, 430–435, Nanchang, China, 2021.

[13] Kivanc, O. C. and S. B. Ozturk, "Sensorless PMSM drive based on stator feedforward voltage estimation improved with MRAS multiparameter estimation," *IEEE/ASME Transactions on Mechatronics*, Vol. 23, No. 3, 1326–1337, Jun. 2018.

[14] Wu, Z. and C. Du, "The parameter identification of PMSM based on improved cuckoo algorithm," *Neural Processing Letters*, Vol. 50, 2701–2715, May 2019.

[15] Zhou, S., D. Wang, and Y. Li, "Parameter identification of permanent magnet synchronous motor based on modified-fuzzy particle swarm optimization," *Energy Reports*, Vol. 9, No. 1, 873–879, Mar. 2023.

[16] Zhang, X., B. Hou, and Y. Mei, "Deadbeat predictive current control of permanent-magnet synchronous motors with stator current and disturbance observer," *IEEE Transactions on Power Electronics*, Vol. 32, No. 5, 3818–3834, May 2017.

[17] Liu, Z.-H., H.-L. Wei, Q.-C. Zhong, K. Liu, and X.-H. Li, "GPU implementation of DPSO-RE algorithm for parameters identification of surface PMSM considering VSI nonlinearity," *IEEE Journal of Emerging and Selected Topics in Power Electronics*, Vol. 5, No. 3, 1334–1345, Sep. 2017.

[18] Xu, W., M. M. Ismail, Y. Liu, and M. R. Islam, "Parameter optimization of adaptive flux-weakening strategy for permanent-magnet synchronous motor drives based on particle swarm algorithm," *IEEE Transactions on Power Electronics*, Vol. 34, No. 12, 12 128–12 140, Dec. 2019.

[19] Liu, Z.-H., H.-L. Wei, X.-H. Li, K. Liu, and Q.-C. Zhong, "Global identification of electrical and mechanical parameters in PMSM drive based on dynamic self-learning PSO," *IEEE Transactions on Power Electronics*, Vol. 33, No. 12, 10 858–10 871, Dec. 2018.

[20] Singh, N. and S. B. Singh, "Hybrid algorithm of particle swarm optimization and grey wolf optimizer for improving convergence performance," *Journal of Applied Mathematics*, Vol. 2017, 2017.

[21] Liu, H. and L. Cao, "Parameter identification of generator excitation system based on improved grey wolf optimization," in *2020 4th International Conference on Electrical, Automation and Mechanical Engineering*, Vol. 1626, No. 1, 012009, Jun. 2020.

[22] Jiang, J. and Z. Zhang, "Multi-parameter identification of permanent magnet synchronous motor based on improved grey wolf optimization algorithm," in *2021 IEEE 4th Student Conference on Electric Machines and Systems (SCEMS)*, 1–7, Huzhou, China, 2021.

[23] Sun, X., Y. Zhang, X. Tian, J. Cao, and J. Zhu, "Speed sensorless control for ipmsms using a modified mras with gray wolf optimization algorithm," *IEEE Transactions on Transportation Electrification*, Vol. 8, No. 1, 1326–1337, Mar. 2022.

[24] Mirjalili, S., S. M. Mirjalili, and A. Lewis, "Grey wolf optimizer," *Advances in Engineering Software*, Vol. 69, 46–61, Mar. 2014.